Modelling and analysis of quench in the 15-kA HTS conductor

Monika Lewandowska[1,2*], Aleksandra Dembkowska[1], Rafał Ortwein[2], Dariusz Bocian[2], Ortensia Dicuonzo[3], Kamil Sedlak[3]

** Corresponding author e-mail: monika.lewandowska@zut.edu.pl*

monika.lewandowska@ifj.edu.pl

[1] Faculty of Mechanical Engineering and Mechatronics, West Pomeranian University of Technology, Szczecin, 70-310 Szczecin, Poland
[2] The Henryk Niewodniczański Institute of Nuclear Physics, Polish Academy of Sciences, 31-342 Krakow, Poland
[3] École Polytechnique Fédérale de Lausanne (EPFL), Swiss Plasma Center (SPC), CH-5232 Villigen PSI, Switzerland

Abstract

High Temperature Superconductors (HTS) are very promising materials for possible application in future fusion magnets and the significant progress in R&D on the respective HTS conductors is observed in recent years. However, since geometric and thermo-physical characteristics of HTS and LTS conductors differ significantly, some doubts have arisen if the approaches successfully used in numerical simulations of the thermal-hydraulic behavior of LTS conductors would be sufficient also for HTS, particularly in cases when fast transient processes (such as e.g. quench) are considered. In order to provide data for better understanding of the quench phenomenon in HTS conductors as well as for testing different numerical approaches and proper tuning of the numerical codes, a dedicated experimental campaign (Quench Experiment) was carried out at the SULTAN test facility within the international collaboration between the EUROfusion consortium and China. Our present study is a part of the work on analysis and interpretation of the data collected during this experiment. Simulations of the selected experimental run were performed using two THEA models with different levels of sophistication. The uncertain model parameters (thermal resistances and copper RRR) were varied in the wide range. The goal of the study was selection of the possibly simple model which would properly reproduce the results of the Quench Experiment.

Keywords: HTS conductors; Quench Experiment; SULTAN test facility; THEA simulations

1. Introduction

High Temperature Superconductors (HTS) are very promising materials to be applied in future fusion magnets [1,2,3,4]. HTS conductors are already considered as a possible option for some components of the superconducting magnet system of the EU DEMO tokamak, which are being designed by the EUROfusion consortium, e.g. for the inner sub-coils of the Central Solenoid developed by the EPFL-SPC team [5,6,7].

Some works on thermal-hydraulic analyses of HTS conductors [7,8,9,10,11] followed the traditional approach, successfully used for Low Temperature Superconductors (LTS), in which all superconducting strands were treated as a single thermal cable component. However, geometric and thermo-physical characteristics of HTS and LTS conductors differ significantly, e.g. only a few thick macro-strands in HTS conductors vs. $\sim 10^3$ thin strands in LTS conductors, quench propagation velocity in HTS much smaller than in LTS, etc. Therefore, it could be expected that numerical simulations of the behavior of HTS conductors may require specific more sophisticated approaches (as attempted e.g. in [12,13,14,15,16]), particularly in cases when fast transient processes (such as e.g. quench) were considered. In order to provide data for better understanding of the quench evolution in HTS conductors as well as for testing different numerical approaches and proper tuning of the uncertain model parameters, a series of dedicated HTS 15-kA sub-size conductors with different geometries were produced and tested by the EPFL-SPC team at the SULTAN test facility in the Quench Experiment [17,18,19], performed within the international collaboration between the EUROfusion Consortium and China, which provided a huge and unique experimental database. Our present work is a part of the work on analysis and interpretation of the results of the Quench Experiment. Other studies on this subject were presented in [20,21]. We simulated a selected experimental run using two THEA models with different levels of complication. Some uncertain model parameters, such as the thermal resistances and copper RRR, were treated parametrically. The goal of the study was the selection of a possibly simple model which would sufficiently well reproduce the results of the Quench Experiment.

2. Quench Experiment

In 2021 four 15-kA sub-size conductors made of a triplet of HTS strands were prepared, as shown schematically in Fig. 1. Each strand was composed of a stack of high-performance second generation (2G) Rare Earth Barium Copper Oxide (REBCO) superconducting tapes, produced by Shanghai Superconducting Technology Co. Ltd. [22], embedded in a cylindrical copper profile.

Each of the two SULTAN samples tested in 2021 consisted of two conductors (either #1 and #2, or #3 and #4), called left leg and right leg, which were electrically connected in series by a joint at the bottom of the sample. Each leg was cooled independently by forced flow of supercritical helium at $p_{in} \approx 10$ bar, $T_{in} \approx 6$ K. The sample was instrumented with a number of temperature sensors (Cernox®) and voltage taps, as presented in Fig. 2. In addition the inlet and outlet temperature and pressure as well as the mass flow rate was measured for each leg.

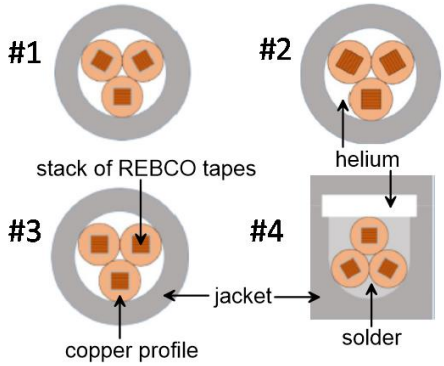

Figure 1. Schematic cross section of the HTS conductors prepared for the Quench Experiment [17]: #1 (reference) with twisted, soldered strands, #2 with twisted, not-soldered strands (tapes are not soldered together), #3 with not-twisted, soldered strands with the tapes wide face perpendicular to the magnetic field (MF), #4 with twisted soldered strands and solder-filled in the space between strands and steel jacket (~135 mm^2 of solder).

The experiment on one sample (two conductors) included two stages: i) DC performance test of the conductors, and ii) Quench Experiment. During the DC test, the critical current (I_c) and the current sharing temperature (T_{cs}) were assessed at various magnetic fields and temperatures, to characterize the conductor and to collect the data for fitting parameters in the $I_c(B,T)$ scaling law. Then the Quench Experiment was performed on each of the two conductors in separate runs. The operating current was ramped up to the desired value. After the steady state was reached, the quench was induced by heating the helium supplied to the conductor either rapidly (several short heat pulses) or slowly. When the warm helium reached the high magnetic field zone (HFZ), the strands temperature could exceed T_{cs} which initiated evolution of a normal zone. If the certain total voltage threshold was reached the current was dumped. Typically the current dump was very fast ($\tau_{dump} \approx 0.1$ s), but there were also few runs with slower ramp-down ($\tau_{dump} \approx 20$ s). The detailed description of the experimental setup and the test campaign is given in [17].

In the present study we focused on the conductor #3 (non-twisted strands with the REBCO tapes wide face perpendicular to the magnetic field) and the run **SPC2 190808** (slow heating, fast current dump) which seemed the simplest for interpretation. The conductor characteristics relevant for our analysis is compiled in Table 1, while the scaling law $I_c(B,T)$ obtained in [17] for this conductor is given by:

$$I_c(B,T) = \frac{A}{B}\left[\frac{B_{irr}(T)}{B_{irr0}}\right]^{\beta}\left[\frac{B}{B_{irr}(T)}\right]^{p}\left[1-\frac{B}{B_{irr}(T)}\right]^{q}, \quad (1a)$$

$$B_{irr}(T) = B_{irr0}\left(1-\frac{T}{T_c}\right)^{\alpha}, \quad (1b)$$

where $A = 4.9494\cdot10^5$ AT, $B_{irr0} = 120$ T, $T_c = 92.83$ K, $\alpha = 2.425$, $\beta = 1.5$, $p = 0.4921$, and $q = 0.5359$.

Table 1. Characteristics of the conductor #3 and its operating conditions considered in our analysis

Description	Unit	Value
Operating current	kA	15
Maximum magnetic field	T	6
Conductor length	m	2.7
Jacket outer diameter	mm	35.3
Jacket thickness	mm	8.5
Number of strands	-	3
Strand diameter	mm	8.5
Stack width	mm	3
Number of HTS tapes	-	3 x 25
Jacket cross section	mm^2	715.3
Copper profiles cross section	mm^2	145.0
REBCO cross section	mm^2	0.225
Copper in tapes cross section	mm^2	4.7
Hastelloy cross section	mm^2	11.3
Silver cross section	mm^2	0.675
$Sn_{40}Pb_{60}$ solder cross section	mm^2	7.6
Helium cross section	mm^2	93.3
Hydraulic diameter	mm	2.8

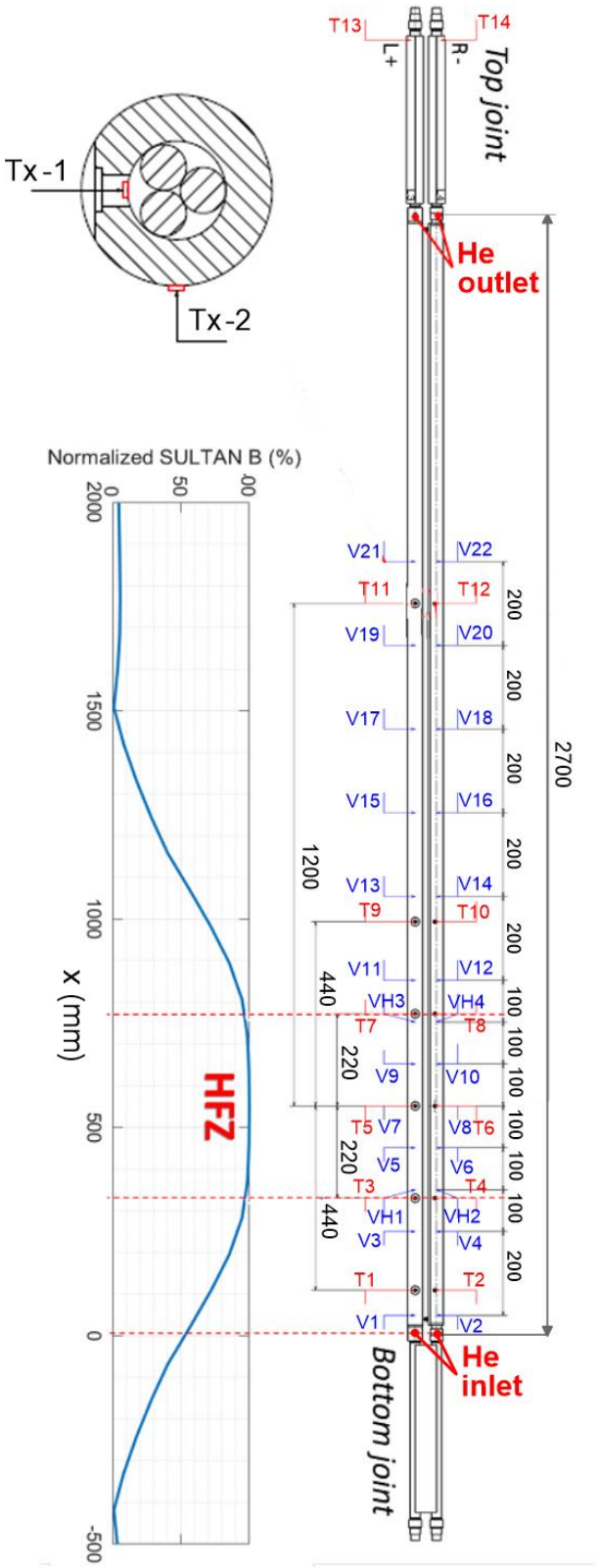

Figure 2. Scheme of the sample instrumentation and the SULTAN magnetic field profile along the sample [17]. The symbol HFZ denotes the high magnetic field zone, where the conductor current sharing temperature is the lowest. Voltage taps and temperature sensors positions are indicated by symbols V and T, respectively. The helium and jacket thermometers are located at the same longitudinal positions Tx of the sample, as shown in the upper left corner.

3. Numerical simulations

We performed, using the THEA code [23,24], simulations of the selected run of the Quench Experiment on the conductor #3 using two models with different levels of geometric complexity.

3.1. The reference THEA model

A THEA model of a conductor consists of several 1D thermal (solid) and hydraulic (fluid) components. In our reference conductor model all strands (HTS stacks + copper profiles) are treated as the first thermal component (Th1) and the jacket is modelled as the second thermal component (Th2), as shown in Fig. 3. Similar simple approach, in which the transverse temperature gradients within the strands and across the jacket are neglected, is typically adopted in thermal-hydraulic analyses of LTS conductors, however, it might not be sufficient for HTS strands with much larger diameters and for relatively thick jacket, as in the considered case.

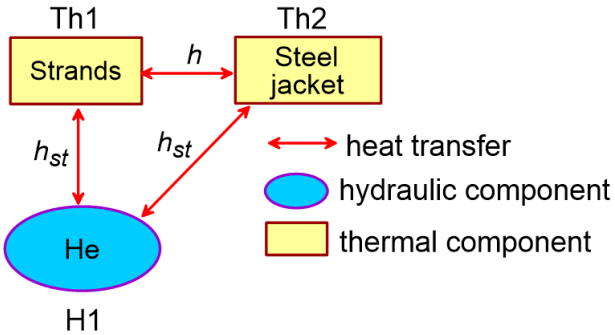

Figure 3. Thermal and hydraulic components in the simple reference THEA conductor model and thermal links between them.

Thermal coupling among two thermal components in THEA is expressed in terms of thermal resistances. We assumed that the strands – jacket thermal resistance is defined as:

$$R_{th} = 1/(h \cdot p_c), \quad (2)$$

where p_c is the strands-jacket contact perimeter (assumed to be 0.5 mm per strand) and h is the respective heat transfer coefficient (contact conductance). The value of h is very uncertain – according to the experimental assessment presented in [25] it can vary in a wide range depending on the surface pressure (from ~250 W/(m^{2}K) at no surface pressure to ~2600 W/(m^{2}K) at 4 MPa). Another uncertain parameter, which strongly affects the Joule heat generation in the normal zone, is the value of copper RRR. There are two copper components in the conductor which may feature different values of RRR: copper layers in the HTS tapes and copper profiles. The latter one, with much larger cross section (see Table 1), has much more significant impact on the quench evolution in the conductor. According to [26], the RRR value of copper in HTS tapes is typically low with a large spread among different tapes investigated (from 3 to 61). We decided to keep the RRR value of copper in tapes constant equal to 53, as in our earlier analyses of the EU-DEMO CS coil [8,11]. The RRR of copper profiles was estimated in [17] to be in the range 40-60, based on resistivity measurements (at 4.2 K, 77 K and 298 K) on three samples taken from the copper profile used to manufacture the strands. In our analysis the values of h and RRR of copper profiles were treated as model parameters,

which should be tuned to obtain the best possible agreement between the simulation and experimental results.

We used the standard smooth tube Dittus-Boelter correlation for the convective helium-jacket and helium-strands heat transfer coefficient (h_{st}). Based on the pressure drop tests of dummy conductors with similar geometry [27] we decided to use the standard Bhatti-Shah smooth tube correlation [28] for the friction factor in the hydraulic component. The adiabatic boundary conditions (constant heat flux equal to zero) were imposed on both ends of the thermal components. For the hydraulic component we intended to formulate the boundary conditions close to the experimental ones. The assumed inlet helium temperature reproduced accurately the readings of the temperature sensor located at the conductor inlet (see Fig. 4).

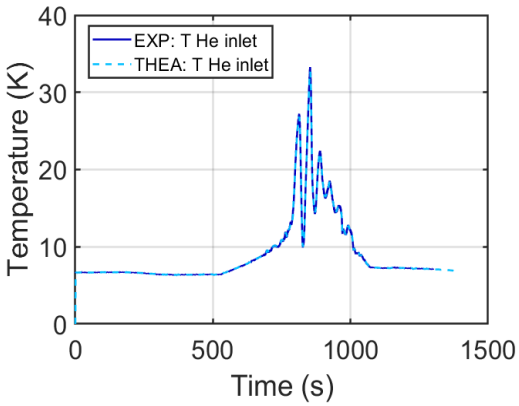

Figure 4. Helium inlet temperature assumed in the THEA model.

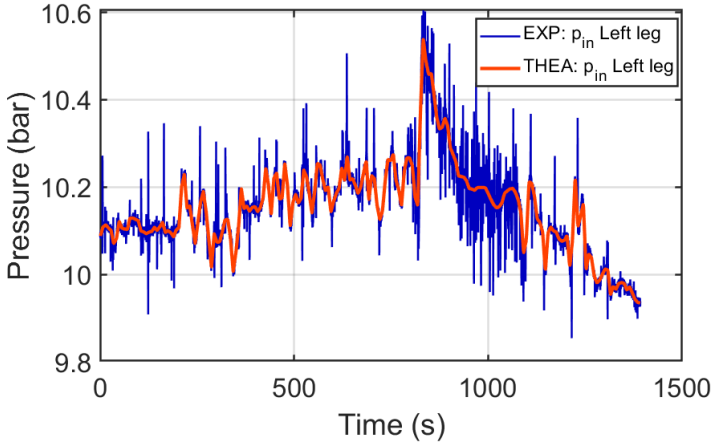

Figure 5. Helium inlet pressure assumed in the second set of boundary conditions used in the THEA model.

We were also attempting to reproduce the readings of the pressure sensors at the conductor inlet and outlet and use them as the boundary conditions in THEA simulations. However, the pressure readings were very noisy and the pressure drop along the sample was much smaller than the level of noise. Moreover, the readings of the pressure sensor at the conductor outlet were typically higher than at the inlet, and despite several attempts to find and subtract an appropriate offset from the p_{out} readings we were unable to reproduce satisfactorily the mass flow rate evolution registered in the experiment with these boundary conditions. Based on the

average value of the steady mass flow rate registered before the start of heating helium ($\dot{m}$ = 1.5 g/s) and using the Bhatti-Shah friction factor correlation we estimated the pressure drop in the sample to be $\Delta p \approx 30$ Pa. In the preliminary simulations we used two sets of pressure boundary conditions: i) constant boundary conditions: p_{in} = 10.2 bar, $p_{out} = p_{in} - \Delta p$, and ii) $p_{in} = p_{in}(t)$, $p_{out}(t) = p_{in}(t) - \Delta p$, where the function $p_{in}(t)$ was obtained by smoothing the readings of the pressure sensor p_{in}, as shown in Fig. 5. In the THEA model we also defined the magnetic field profile (Fig. 6) and time evolution of the operating current reproducing the experimental conditions.

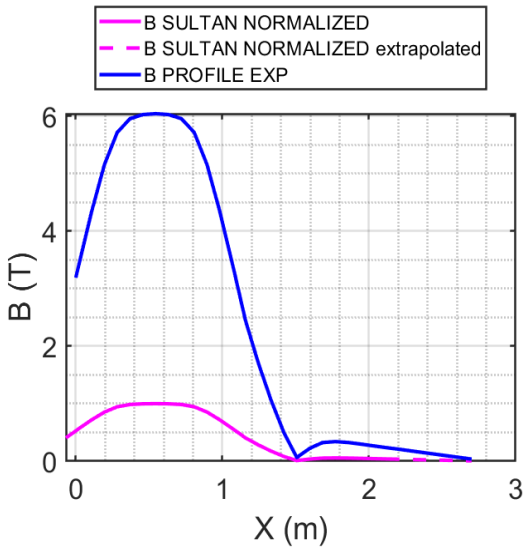

2.

Figure 6. Magnetic field profile along the conductor implemented in the THEA model.

3.2. Results obtained with the reference THEA model

We performed parametric simulations of the experimental run SPC2 190808 for different pairs of values h and RRR of copper profiles. We started with the conservative values of RRR = 40 and h = 500 W/(m^{2}K), which were close to the lowest values observed in the experiments [17,25]. It is worth to mention that this value of h is typically used in thermal – hydraulic analyses of EU-DEMO coils, as agreed by the WPMAG project team [29]. The whole set of (h/R_{th}, RRR) pairs for which we performed simulations of the run SPC2 190808 with the reference THEA model is listed in Table 2.

Some typical results of the simulations obtained with the reference THEA model are presented in Figs. 7-9. Three trends in time evolution of the mass flow rate and temperatures can be noticed. As shown in Fig. 8, for several pairs of (R_{th} ,RRR,), marked in Table 2 with the "o" symbol, e.g. (0.167 mK/W, 40), (1.33 mK/W, 80), the qualitative shape of mass flow rate and temperatures time evolution was captured correctly. Also quantitatively, the experimental mass flow rate as well as the jacket and He temperatures close to the conductor inlet (locations 1 and 3) agreed reasonably well with the simulations results. However, the values of temperatures at other locations (5, 7, 9, 11 and outlet) and the total voltage (Fig. 8b) obtained from simulations were much lower than the respective experimental results.

For all pairs of (R_{th}, RRR), marked in Table 2 with the symbol "v", the temperatures and voltage values resulting from simulations were even smaller than in previous case (see some examples in Figs. 9). Also the conductor recooling time was shorter than in the experiment. For some pairs of (R_{th}, RRR), marked in Table 2 with the symbol "x", the mass flow rate, temperature and voltage values obtained from simulations were close to experiment but only before the start of the current dump. However, in all these cases the simulation results for the recooling phase were far from the experiment (see some examples in Figs. 7).

Table 2. Pairs of values of the contact conductance/thermal resistance (h/R_{th}) and RRR of copper profiles for which we performed simulations with the reference THEA model. The pairs of parameters for which the results are presented in Figs. 7-9 are marked in bold.

h W/(m^{2}K)	R_{th} (mK/W)	RRR (-)				
		40	55	60	80	100
500	1,333	**x**	x	x	o	v
1200	0,555	x		o		
2000	0,333			x		
4000	0,167	**o**		v		
6000	0,111	**v**		v	v	v
8000	0,083			v		

Increasing of the RRR value reduces the Joule heat generation occurring for I > 0 in the normal zone. Increasing the h value (reduction of R_{th}) leads to a similar effect, because it enhances heat transfer from the strands to the jacket at the early stage of the quench evolution, and thus reduces the strands temperature and their resistivity. There are many pairs of (R_{th}, RRR) values for which the simulation results are almost identical, even if we restrict the RRR values of copper profiles to the experimental range 40-60 [17]. This makes the reliable tuning of the model parameters problematic.

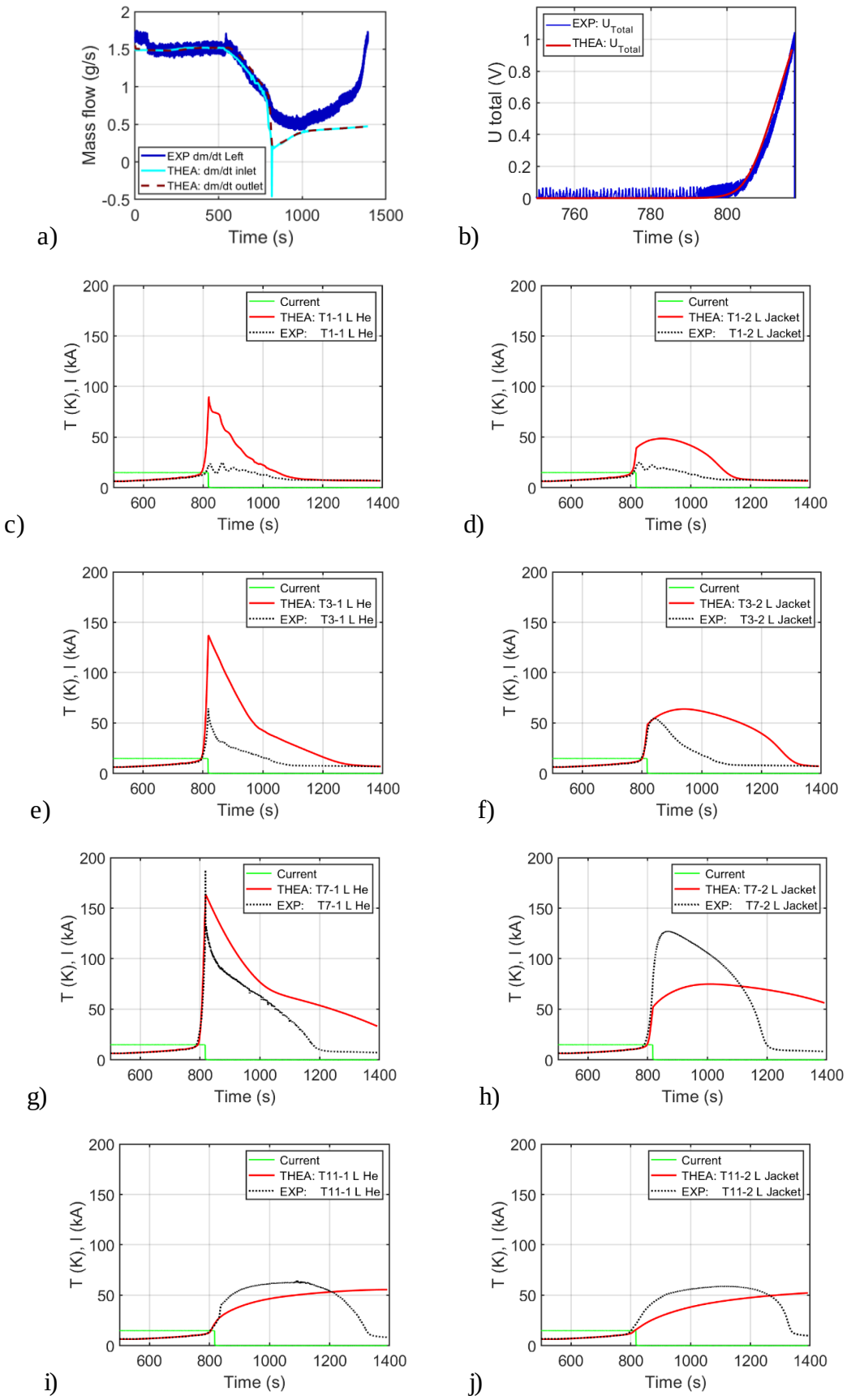

Figure 7. Comparison of the experiment and the simulation results obtained with the THEA reference model for h = 500 W/(m^{2}K) (R_{th} = 1.333 mK/W), RRR =40, p_{in} = 10.2 bar = const.

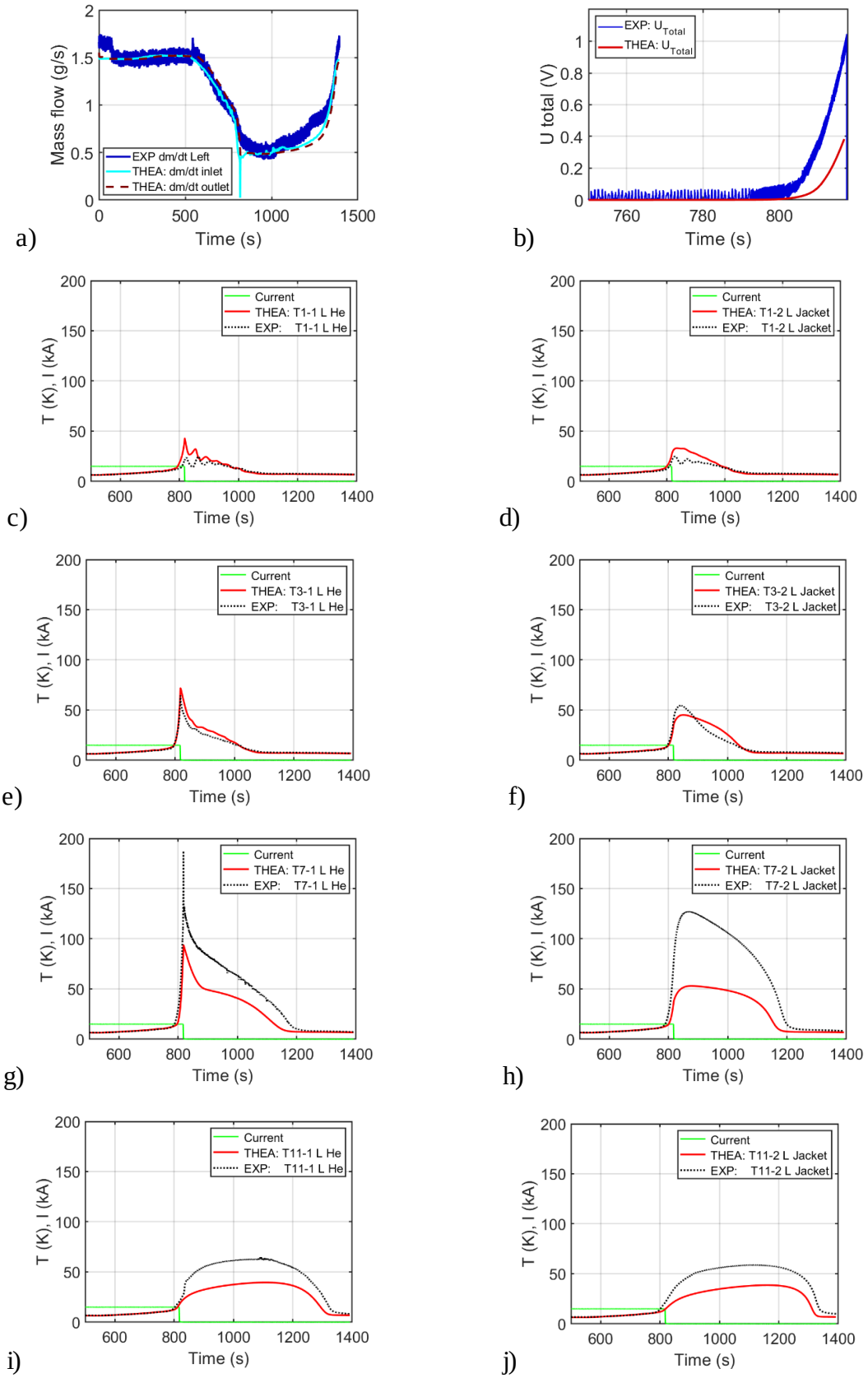

Figure 8. Comparison of the experiment and the simulation results obtained with the THEA reference model for h = 4000 W/(m^{2}K) (R_{th} = 0.167 mK/W), RRR =40, p_{in} = 10.2 bar = const. Almost identical results were obtained for other (h/R$_{th}$, RRR) pairs, e.g. h = 500 W/(m^{2}K) (R_{th} = 1.333 mK/W) and RRR=80, or h = 1200 W/(m^{2}K) (R_{th} = 0.555 mK/W) and RRR=60.

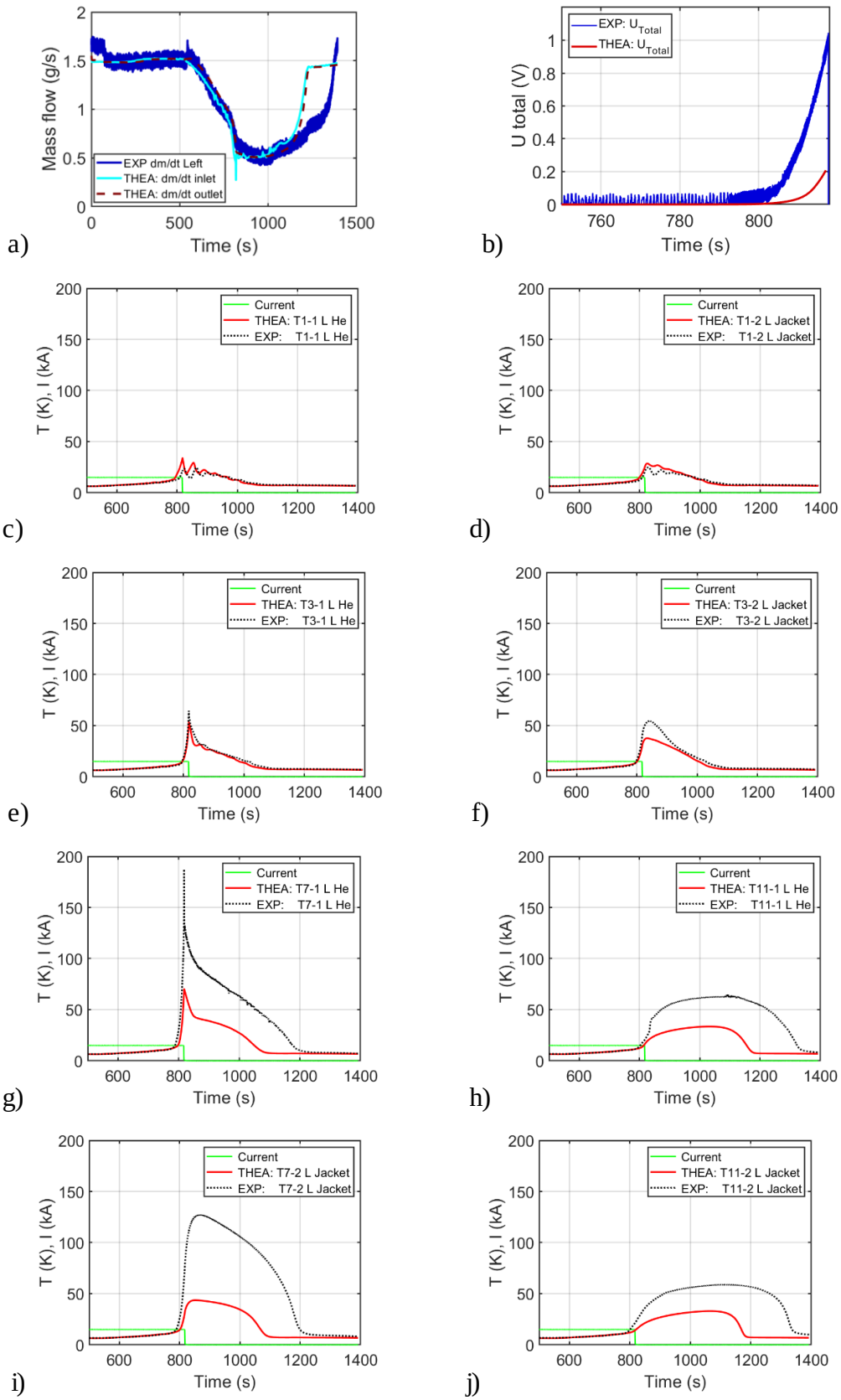

Figure 9. Comparison of the experiment and the simulation results obtained with the THEA reference model for h = 6000 W/(m^{2}K) (R_{th} = 0.111 mK/W), RRR =40, p_{in} = 10.2 bar = const.

All the simulations discussed above were performed with constant pressure boundary conditions: p_{in} = 10.2 bar, $p_{out} = p_{in} - \Delta p$. Afterwards, we repeated several simulations using the variable pressure boundary conditions $p_{in} = p_{in}(t)$ (see Fig. 5), $p_{out} = p_{in} - \Delta p$. We observed that this change of the pressure boundary condition had no noticeable impact on the results, except disappearance of the flow instability observed in simulations with the constant boundary conditions at the end of the current dump (compare Figs. 7a and 10). Because of this improvement further simulations were carried out with the variable pressure boundary condition.

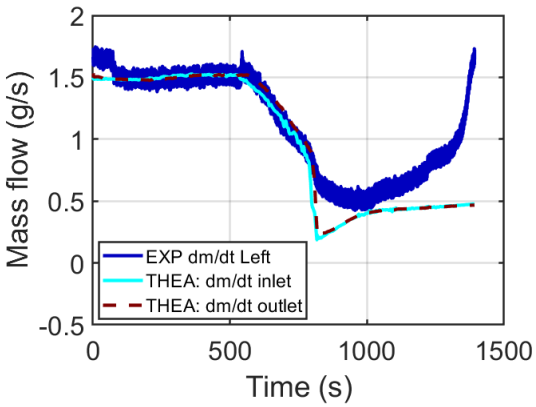

Figure 10. Comparison of the mass flow rate resulting from the experiment and from the simulation with the THEA reference model for h = 500 W/(m^{2}K) (R_{th} = 1.333 mK/W), RRR =40, $p_{in} = p_{in}(t)$.

The reference model, in which all strands and thick jacket were treated as two thermal components, confirmed to be insufficient for reliable simulations of quench in the considered HTS conductor. Therefore we formulated an extended THEA model in which we made an attempt to take into account the radial temperature gradient in the jacket.

3.3. The extended THEA model

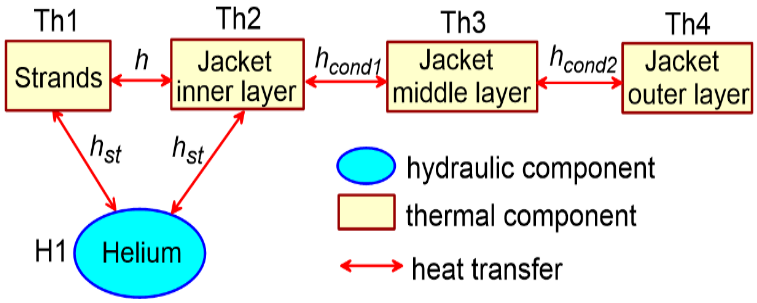

Figure 11. Thermal and hydraulic components in the extended THEA model of the conductor and thermal links between them.

In the extended model (shown schematically in Fig. 11) the conductor jacket was split into three thermal components: the inner layer (thickness 0.2 mm), the middle layer (thickness 8.1 mm), and the outer layer (thickness 0.2 mm). The Th2-Th3 and Th3-Th4 thermal resistances, resulting from heat conduction through cylindrical walls, were defined as:

$$R_{th1} = \frac{\ln\left(\frac{d_2}{d_1}\right)}{2\pi k_{steel}\left(T_{av1}\right)}, \tag{3a}$$

$$R_{th2} = \frac{\ln\left(\frac{d_3}{d_2}\right)}{2\pi k_{steel}\left(T_{av2}\right)}, \tag{3b}$$

where k_{steel} is the steel thermal conductivity, calculated at the average temperature of the respective thermal components ($T_{av1}(x, t) = (T_{Th2}(x, t) + T_{Th3}(x, t))/2$, $T_{av2}(x, t) = (T_{Th3}(x, t) + T_{Th4}(x, t))/2$), and the mean diameters of the subsequent jacket layers (d_1, d_2 and d_3) are defined in Fig. 12. The rest of the model assumptions was the same as in the reference THEA model (see section 3.1).

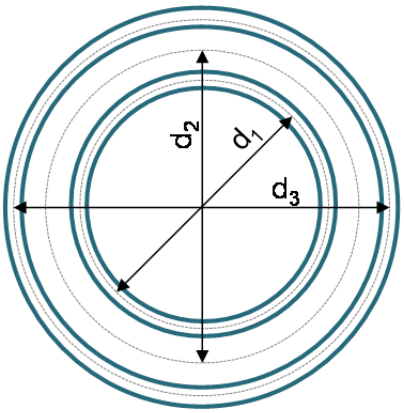

Figure 12. Definition of diameters d_1 - d_3 in Eqs. (3) (not in scale).

Similar approach was adopted in our earlier THEA simulations of another thermal-hydraulic experiment, (in which the heat flux transferred by heat conduction through a conductor jacket was known) and provided the temperature difference on both sides of the jacket wall consistent with the analytical calculations [30]. Splitting the 10-mm-thick conduit into 10 thermal components, corresponding to the subsequent concentric cylindrical steel shells, was also applied in THEA simulations of other quench experiment, which resulted in reasonable values of the hot spot temperature [31].

3.4. Results obtained with the extended THEA model

The whole set of (h/R_{th}, RRR) pairs for which we performed simulations of the run SPC2 190808 with the extended THEA model is compiled in Table 3, whereas typical results of the simulations are presented in Figs. 13-15.

A striking feature of the extended THEA model is that for a given pair of parameters (h/R_{th}, RRR) it predicts much higher helium and jacket temperatures than the reference THEA model (see Figs. 8 and 13). This is because in the extended THEA model the temperature of the jacket inner layer at a given location is higher than the respective average jacket temperature in the reference THEA model, which results in reduction of helium-jacket heat transfer, and

consequently also deterioration of heat removal from the strands. Three typical trends similar to those observed in the results of simulations with the reference THEA model (discussed in section 3.2) can be noticed again in the results of the extended THEA model (Figs. 13-15). However, in the extended THEA model, the line in the (h/R_{th}, RRR) parameter space for which the conductor recooling time obtained from the simulations agrees with experiment (marked in Tables 2 and 3 with symbol "o") is clearly shifted towards higher h and RRR values w.r.t. the reference THEA model. Thus, to obtain the proper recooling time in the simulations with the extended THEA model, for RRR in the experimental range (40-60 [17]), we need to assume the h value of at least 7000 W/(m^{2}K) (see the results for RRR = 60 and h = 7000 W/(m^{2}K) (R_{th} = 0.095 mK/W) in Fig. 15), which is much higher than the experimental h values obtained in [25]. However, it is possible that the actual strands – jacket surface pressure in the quench experiment was larger than 4 MPa reached in the experiment presented in [25]. Another possible explanation could be the underestimation of the strands-jacket contact perimeter assumed in our analysis. It is also likely that both the contact perimeter and the contact conductance were not constant during the quench experiment, but they could increase when the strands temperature was higher than the jacket temperature due to the thermal expansion of the strands. In further analyses of the Quench Experiment introduction of the thermal resistance R_{th} dependent on the temperature difference between the strands and the jacket could be considered.

It should be noticed that in the extended THEA model, in the cases where the conductor recooling time was reproduced properly, the temperatures and total voltage were noticeably closer to the respective experimental values than in the reference model (see Figs. 8 and 15), being an improvement. Further extension of the THEA model by splitting strands into 2 thermal components (HTS stacks and copper profiles) would be interesting.

Table 3. Pairs of values of the contact conductance/thermal resistance (h/R_{th}) and RRR of copper profiles for which we performed simulations with the reference THEA model. The pairs of parameters for which the results are presented in Figs. 13- 15 are marked in bold.

h W/(m^{2}K)	R_{th} (mK/W)	RRR (-)			
		40	60	80	100
2000	0,333			x	o
4000	0,167	**x**	x	o	**v**
6000	0,111		x	v	
7000	0,095		**o**	v	

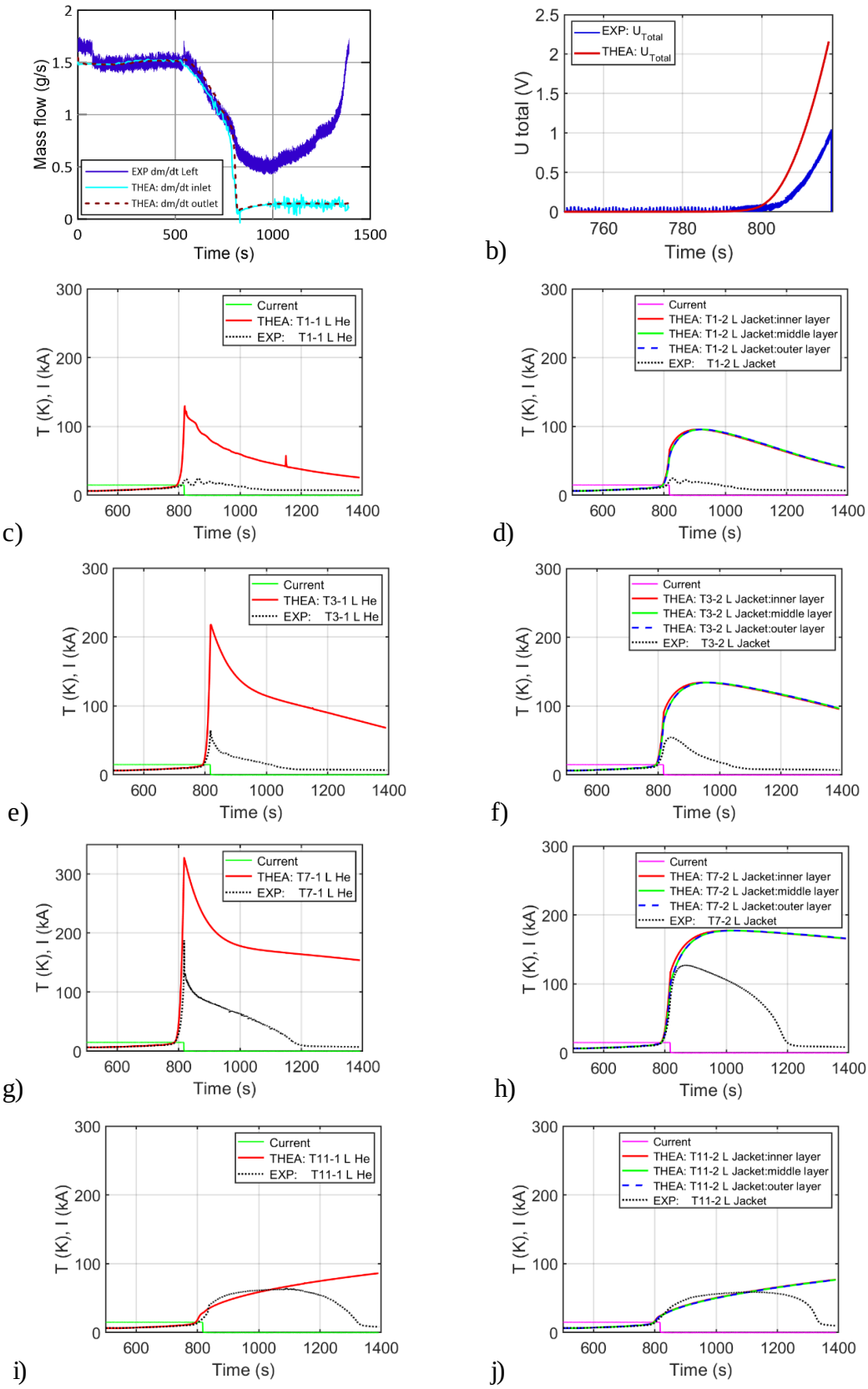

Figure 13. Comparison of the experiment and the simulation results obtained with the THEA extended model for h = 4000 W/(m^{2}K) (R_{th} = 0.167 mK/W), RRR =40, $p_{in} = p_{in}(t)$.

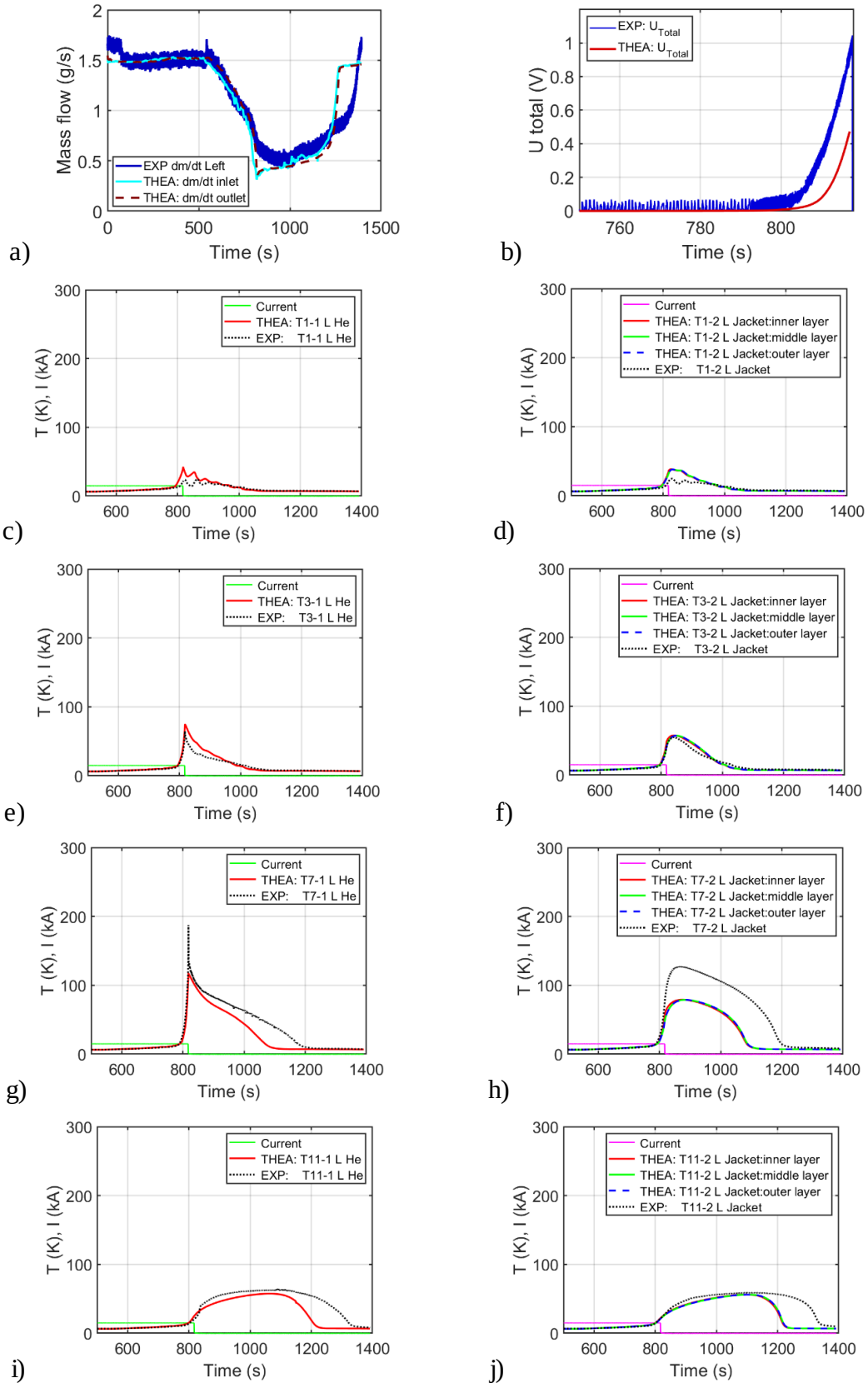

Figure 14. Comparison of the experiment and the simulation results obtained with the THEA extended model for h = 4000 W/(m^{2}K) (R_{th} = 0.167 mK/W), RRR =100, $p_{in} = p_{in} = p_{in}$ (t).

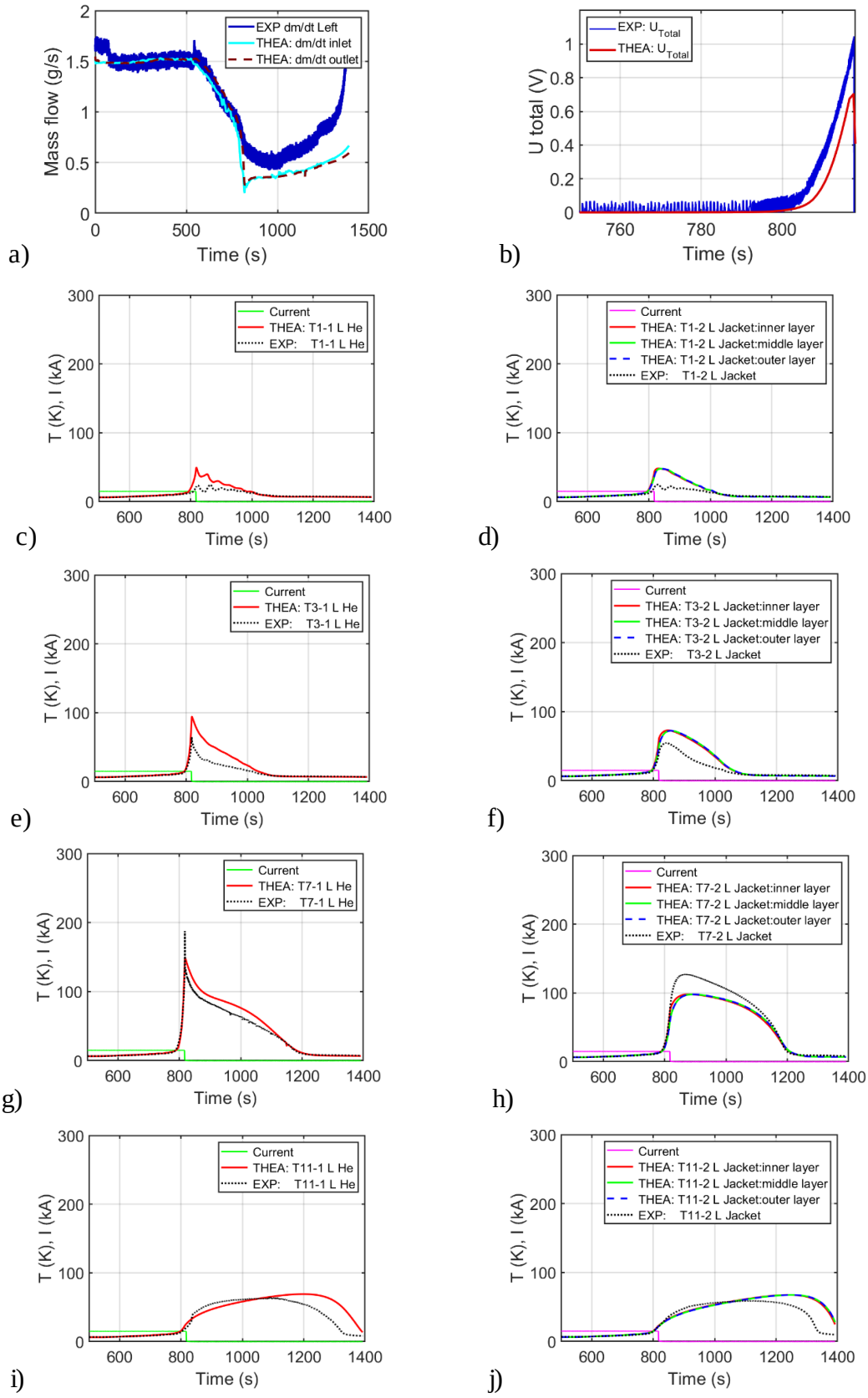

Figure 15. Comparison of the experiment and the simulation results obtained with the THEA extended model for h = 7000 W/(m^{2}K) (R_{th} = 0.095 mK/W), RRR =60, $p_{in} = p_{in}(t)$. Similar results were obtained for other (h/R_{th}, RRR) pairs: h = 2000 W/(m^{2}K) (R_{th} = 0.333 mK/W) and RRR = 100, or h = 4000 W/(m^{2}K) (R_{th} = 0.167 mK/W) and RRR=60.

4. Summary, conclusions and perspectives

The Quench Experiment on several sub-size 15-kA HTS conductors was performed by the EPFL-SPC team in 2021 [17]. We created two THEA models of the sample #3, namely: the reference THEA model (all strands and the jacket treated as two thermal components), and the extended model (with the jacket split into 3 thermal components), which were used for simulations of the selected run of the quench experiment for the wide range of values of the uncertain model parameters (RRR of copper profiles and strands-jacket thermal conductance (or the respective thermal resistance R_{th})).

We observed, that for several considered pairs of values (R_{th} , RRR), namely:

- (0.167 m·K/W, 40), (0.555 m·K/W, 60), (1.333 m·K/W, 80) in the reference THEA model,
- (0.095 m·K/W, 60), (0.167 m·K/W, 80), (0.333 m·K/W, 100) in the extended THEA model (only the first of these pairs has the RRR in the experimental range [17]),

the experimental time evolution of the mass flow rate as well as the conductor recooling time were reproduced well by the simulations' results. However, in the reference model the temperatures (particularly at the locations 7, 9, 11 and T_{out}) and the total voltage were much lower than the respective experimental readings, only the qualitative shape of these time characteristics was captured correctly. The overall agreement of the simulation with the data was improved in the extended model, however, the voltage values were still slightly smaller than in the experiment. If the values of (R_{th}, RRR) were tuned to reproduce well the voltage evolution, other thermal-hydraulic characteristics (mass flow rate and temperature evolution, particularly during the recooling phase) were far from the experiment (particularly in the reference model).

The reference model confirmed to be insufficient for reliable simulations of quench in the considered HTS sample, although such an approach is usually successfully applied for LTS conductors. As a next step, splitting the strands into 2 thermal components (copper profiles + HTS stacks) and introducing temperature dependent h/R_{th} could be considered.

References

[1] W.H. Fietz, Ch. Barth, S. Drotziger, W. Goldacker, R. Heller, S.I. Schlachter, K.-P. Weiss, Prospects of high temperature superconductors for fusion magnets and power applications. Fusion Eng. Des. 88 (2013) 440–5.

[2] W.H. Fietz, M.J. Wolf, A. Preuss, R. Heller, K.-P. Weiss, High-current HTS cables: status and actual development. IEEE Trans. Appl. Supercond. 26 (2016) Art. no. 4800705.

[3] P. Bruzzone, W.H. Fietz, J.V. Minervini, M. Novikov, N. Yanagi, Y. Zhai, J. Zheng, High temperature superconductors for fusion magnets. Nucl. Fusion 58 (2018) Art. no. 103001.

[4] M.J. Wolf, C. Ebner, W.H. Fietz, R. Heller, D. Nickel, K.-P. Weiss, High temperature superconductors for fusion applications and new developments for the HTS CroCo conductor design. Fusion Eng. Des. 172 (2021) Art. no. 112739.

[5] R. Wesche, X. Sarasola, K. Sedlak, N. Bykovskiy, B. Stepanov, D. Uglietti, P. Bruzzone, DEMO central solenoid design based on the use of HTS sections at highest magnetic field, IEEE Trans. Appl. Supercond. 28 (2018), 4203605.

[6] R. Wesche, X. Sarasola, O. Dicuonzo, I. Ivashov, K. Sedlak, D. Uglietti, P. Bruzzone, Hybrid HTS-Nb_3Sn-NbTi DEMO CS coil design optimized for maximum magnetic flux generation, Fusion Eng. Des. 146 (2019) 10–13.

[7] R. Guarino, M. Lewandowska, A. Dembkowska, N. Bykovskiy, X. Sarasola, K. Sedlak, Thermal-hydraulic analysis of alternative cable-in-conduit conductors for the European DEMO hybrid central solenoid. Fusion Eng. Des. 187 (2023) Art. no. 113368.

[8] A. Dembkowska, M. Lewandowska, X. Sarasola, Thermal-Hydraulic Analysis of the DEMO CS Coil. IEEE Trans. Appl. Supercond. 28 (2018) Art. no. 4205605.

[9] M. Lewandowska, A. Dembkowska, R. Heller, M. Wolf, Thermal-hydraulic analysis of an HTS DEMO TF coil. Cryogenics 96 (2018) 125-32.

[10] R. Heller, P. Blanchier, W. H. Fietz, M.J. Wolf, Quench Analysis of the HTS CrossConductor for a Toroidal Field Coil. IEEE Trans. Appl. Supercond. 29 (2019) Art. no. 4703111

[11] A. Dembkowska, M. Lewandowska, X. Sarasola, K. Sedlak, Quench analysis of the DEMO CS1 coil. Cryogenics 112 (2020) Art. no. 103194.

[12] M. Wolf, R. Heller, W.H. Fietz, K.-P. Weiss, Design and analysis of HTS subsize conductors for quench investigations towards future HTS fusion magnets. Cryogenics 104 (2019) Art. No. 102980.

[13] A. Zappatore, W.H. Fietz, R. Heller, L. Savoldi, M.J. Wolf, R. Zanino, A critical assessment of thermal–hydraulic modeling of HTS twisted stacked-tape cable conductors for fusion applications. Supercond. Sci.Technol. 32 (2019) Art. no. 084004.

[14] R. Kang, D. Uglietti, Y. Song, Modelling quench of a 50 kA REBCO conductor with soldered-twisted-stacked-tape-cable strands. Cryogenics 106 (2020) Art. no. 103037.

[15] R. Kang, D. Uglietti, R. Wesche, K. Sedlak, P. Bruzzone, Y. Song, Quench Simulation of REBCO Cable-in-Conduit Conductor with Twisted Stacked-Tape Cable. IEEE Trans. Appl. Supercond. 30 (2020) Art. no. 5700107.

[16] R. Kang, D. Uglietti, Y. Song, To the Optimization of Quench Performance for a Large REBCO Cable-in-Conduit Conductor. IEEE Trans. Appl. Supercond. 31 (2021) Art. no. 4600209.

[17] O. Dicuonzo, Electromechanical investigations and quench experiments on sub-size HTS cables for high field EU-DMO Central Solenoid. PhD Thesis, EPFL-SPC 2022.

[18] O. Dicuonzo, R. Kang, K. Sedlak, B. Stepanov, D. Uglietti, R. Wesche, P. Bruzzone, Upgrade and Commissioning of the SULTAN Facility to Host Quench Experiments on HTS High Current Conductors. IEEE Trans. Appl. Supercond. 31 (2021) Art. no. 9500505.

[19] N. Bykovskiy, H. Bajas, O. Dicuonzo, P Bruzzone, K. Sedlak, Experimental study of stability, quench propagation and detection methods on 15 kA sub-scale HTS fusion conductors in SULTAN, Supercond. Sci. Technol. 36 (2023) Art. no. 034002.

[20] A . Zappatore, R. Bonifetto, P. Bruzzone, V. Corato, O. Dicuonzo, M. Kumar, K. Sedlak, B. Stepanov, Quench experiments on sub-size HTS Cable-In-Conduit Conductors for fusion applications: Data analysis and model validation. Cryogenics 132 (2023) 103695.

[21] A. Zappatore, R. Bonifetto, R. Zanino, Analysis and modelling of the quench experiment on HTS sub-sized cable-in-conduit conductors for fusion applications. Presented at CHATS-AS 2023, 3-5.05.2023, Torino

[22] Shanghai Superconducting Technology Co. Ltd., Shanghai, China. http://www.shsctec.com .

[23] L. Bottura, C. Rosso, M. Breschi, A general model for thermal, hydraulic and electric analysis of superconducting cables. Cryogenics 40 (2000) 617–26.

[24] THEA—Thermal, Hydraulic and Electric Analysis of Superconducting Cables. User's Guide Version 2.3, CryoSoft, 2016. https://supermagnet.sourceforge.io/manuals/Thea_2.3.pdf.

[25] K. Takahata, H. Tamura, T. Mito, Thermal Contact Conductance Between the Bundle and the Conduit in Cable-in-Conduit Conductors. IEEE Trans. Appl. Supercond. 14 (2004) 1477-1480.

[26] J. Fleiter, K. Konstantopoulou, D. Richter, A. Ballarino, Characterization of REBCO Tape and Roebel Cable at CERN. 4th Workshop on Workshop on Accelerator Magnets in HTS (WAMHTS-4) Barcelona, 15th February 2017.

[27] M. Lewandowska, A. Dembkowska, R. Heller, J. Świerblewski, M. Wolf, Hydraulic characterization of conductor prototypes for fusion magnets. Cryogenics 110 (2020) Art. no. 103013.

[28] R.K. Shah, D.P. Sekulić. Fundamentals of Heat Exchanger Design. New Jersey: Wiley; 2003, pp. 476–83.

[29] V. Corato, et al., Common operating values for DEMO magnets design for 2016. http://www.euro-fusionscipub.org/archives/eurofusion/common-operating-values-for-demo-magnets-design-for-2016-2

[30] M. Lewandowska, A. Dembkowska, P. Herbin, L. Malinowski: Steady-state transverse heat transfer in a single channel CICC. Cryogenics 110 (2020) Art. no. 103124.

[31] K. Sedlak, P. Bruzzone, Results and analysis of the hot-spot temperature experiment for a cable-in-conduit conductor with thick conduit. Cryogenics 72 (2015) 9-13.